BIOCHEMISTRY
including biophysical chemistry & molecular biology

ARTICLE

pubs.acs.org/biochemistry

Light-Induced Conformational Changes in Photosynthetic Reaction Centers: Impact of Detergents and Lipids on the Electronic Structure of the Primary Electron Donor

S. S. Deshmukh,[†] H. Akhavein,[†] J. C. Williams,[‡] J. P. Allen,[‡] and L. Kálmán*[,†]

[†]Department of Physics, Concordia University, Montreal, Quebec H4B 1R6, Canada

[‡]Department of Chemistry and Biochemistry, Arizona State University, Tempe, Arizona, 85287-1604, United States

ABSTRACT: Light-induced hypsochromic shifts of the Q_y absorption band of the bacteriochlorophyll dimer (P) from 865 to 850 nm were identified using continuous illumination of dark-adapted reaction centers (RCs) from *Rhodobacter capsulatus* when dispersed in the most commonly used detergent, the zwitterionic lauryl *N*-dimethylamine-*N*-oxide. Such a shift is known to be the consequence of the decreased degree of delocalization of P. A 2-fold acceleration of the recovery kinetics of P^+ was found in RCs that underwent light-induced structural changes compared to those where the P-band position did not change. The light-induced shift was irreversible except in the presence of a secondary electron donor. Prolonged (15 min) illumination resulted in a shift in the position of the P-band even in neutral or negatively charged detergents. In contrast, RCs reconstituted into liposomes made from lipids with different headgroup charges showed light-induced shifts only if shorter fatty acid chains were used. The light-induced conformational changes caused a prominent decrease of the redox potential of P ranging from 120 to 160 mV depending on the detergent compared to the potential of P in dark-adapted reaction centers. The measured light-induced potential decreases were 55 to 85 mV larger than those reported for reaction centers where the P-band position remained at 865 nm. The influence of structural factors, such as the delocalization of the electron hole on P^+, the involvement of Tyr M210, and the hydrophobic mismatch between the thickness of the hydrophobic belt of the detergent micelles or the lipid bilayer and the RC protein, on the spectral features and electron transfer kinetics is discussed.

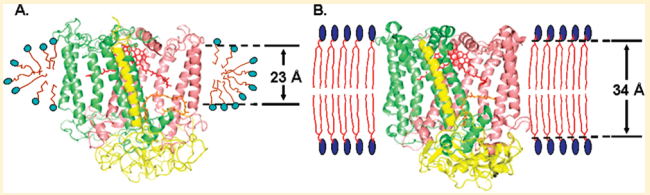

The reaction center (RC) of purple non-sulfur bacteria is the site for the conversion of light energy into a transmembrane charge separation over a ~30 Å distance.[1] Upon light excitation, the primary electron donor (P), a special pair of two bacteriochlorophyll molecules, transfers an electron via one of the monomeric bacteriochlorophyll (B_A) and bacteriopheophytin (H_A) molecules to the primary quinone (Q_A) and then to the secondary quinone (Q_B). The RC has three polypeptides, L, M, and H, of which the L and M subunits bind noncovalently two branches of cofactors, (P, B, H, and Q molecules), a non-heme Fe^{2+}, and a carotenoid.[2] The structure of the RC from *Rhodobacter* (*Rba.*) *capsulatus* has not been determined, but it is presumed to be very similar to the structure of the RC from *Rba. sphaeroides* based on the amino acid sequence similarity between the two species.[3−6] Despite the approximate 2-fold symmetry in the cofactor arrangement, electrons are transferred only along one of the two branches.[7] The kinetics and the energetics of charge separation are determined by the oxidation−reduction potentials and electronic couplings of the individual electron donor and acceptor pairs according to Marcus theory.[8] The local protein environment tunes the potential of the otherwise identical molecules, making only one of the two branches energetically accessible for the transmembrane charge separation.[9]

The overwhelming majority of the accumulated knowledge about the structure and the coupling between the electron and proton transfer reactions has been obtained using RCs that were purified in detergents to substitute for the natural membrane environment. The isolation procedure and the selection of the detergent has been found to significantly alter the spectroscopic properties of the RC.[10−12] Several studies have emphasized that the kinetics and thermodynamics of the electron transfer reactions have drastically different features in chromatophores (native membrane fragments), which is the closest match to the conditions *in vivo*. For example, the electron transfer reactions between the quinones and the charge recombination between Q_A^- and P^+ have been found to occur significantly faster in the native membrane than in detergent micelles.[13,14] This trend was recently confirmed in a study where intact cells were used.[15] Contrarily, a 2−3-fold slower charge recombination reaction between Q_B^- and P^+ was reported in chromatophores than in detergent micelles.[16] The charge recombination from Q_B^- in detergent micelles occurs using the indirect route via Q_A^-, while in chromatophores the direct route is predominant.

Received: April 19, 2011
Revised: May 11, 2011
Published: May 11, 2011

As part of the stabilization, in detergent isolated reaction centers the formation of either semiquinone is accompanied by a substoichiometric proton uptake by residues interacting with the semiquinones in both *Rba. sphaeroides* and *Rba. capsulatus*.[17−19] In contrast, in chromatophores of *Rba. capsulatus* direct protonation of Q_B^- has been observed.[14] It was concluded that the free energy differences between the redox cofactors have been altered by the replacement of the membrane with detergents due to the differences in the electrostatic interactions between the cofactors and the polar or charged headgroup of the detergent or the lipid. However, the differences between the observed behavior of the RCs in detergent micelles and in native or artificial lipid bilayers were not scrutinized in terms of hydrophobic interactions.

Kinetic studies of light-induced absorption changes have detected at least two populations of the RCs if exposed to continuous illumination with significantly different stabilities of the charge-separated states in *Rba. sphaeroides*.[20−28] In most of the earlier spectroscopic studies, a dual conformational model was proposed to account for the two major spectral populations of the RCs that were modeled in terms of a dark- and light-adapted conformation. Most groups have focused their attention to the cytoplasmic side of the RCs near the quinones to identify the structural changes at the molecular level.[20,22−25] The Q_B cofactor exchanges with the exogenous quinone pool after two electron and proton transfer events necessitating it to be mobile and sensitive to the protonation state of local side chains. In addition, light-induced structural changes were reported near the quinones based on crystallographic studies.

Our very recent studies conducted on RCs from site directed mutants that have different hydrogen-bonding patterns between P and the surrounding protein isolated from *Rba. sphaeroides* presented evidence that structural changes near P are responsible for the very long lifetime of the charge-separated state after prolonged illumination.[27,28] A correlation between the type of mutation and several electronic properties, including the redox midpoint potential of P, the light-induced electrochromic absorption changes of the bands of the nearby B molecules due to the increase of the local dielectric constant, and proton release from the periplasmic side, was interpreted in terms of structural changes of P and its local environment. In this work, these studies on RCs from *Rba. sphaeroides* have been extended to RCs from *Rba. capsulatus*, which shows pronounced spectral changes depending upon the choice of detergents. While in their native membranes the peak position of the Q_y absorption band of P in both *Rba. sphaeroides* and *Rba. capsulatus* is centered at 865 nm, this position of the P band in RCs from *Rba. capsulatus* has been reported to be affected by the zwitterionic *N*-lauryl-*N*,*N*-dimethylamine-*N*-oxide (LDAO), which is the most commonly used detergent for RC isolation and characterization.[29] When RCs are purified using LDAO, the peak position of the P-band in *Rba. sphaeroides* stays at 865 nm, but it was reported to be downshifted by 15 nm in *Rba. capsulatus* to 850 nm. These positions can be systematically switched by selecting detergents with different headgroup charges in both strains.[29,30] This spectroscopic difference was identified earlier as an indicator for two different electronic structures of P.[30] Here, the effects of prolonged, continuous illumination on the Q_y absorption band of P in RCs from *Rba. capsulatus* are measured using steady-state and transient optical spectroscopy in both detergent micelles and in lipid bilayers. In particular, the light-induced conversion between different spectral states, which has not been reported previously, is investigated. These optical shifts are characterized in terms of structural changes of P involving electrostatic and hydrophobic interactions with the surrounding membrane substituent and compared to those observed for RCs from *Rba. sphaeroides*.

EXPERIMENTAL PROCEDURES

Bacterial Growth and Reaction Center Isolation. An antennaless strain of *Rba. capsulatus* was used that was constructed from U43, in which the *puf* operon including the RC and the light-harvesting complex (LHC) I (B875) genes were deleted and the LHC II (B880-850) was lost by a chromosomal point mutation.[31] The wild-type genes were carried on a derivative of the plasmid pU2922 and conjugated into the deletion strain.[32] On this plasmid a putative bacteriochlorophyll binding ligand, His 32 of LHC I, was changed to Arg.[33] The bacteria were grown in RCV-PY medium semiaerobically as described earlier.[34] The RCs were isolated and purified according to the procedure introduced by Bylina and Youvan and later were dispersed in 0.05% LDAO.[33] The purity of the RCs, defined as the ratio of the absorbance at 280 to 802 nm, was typically between 1.8 and 2.5 for all preparations used in this study. The wild-type strain from *Rba. sphaeroides* was grown under nonphotosynthetic conditions, and the RCs were isolated and purified using procedures described previously.[35] For some experiments the LDAO detergent was replaced with the neutral detergent Triton X-100 (TX-100) and the negatively charged detergent deoxycholate (DOC) by extensive dialysis of the samples. The RCs appeared to be not stable if similar dialysis was attempted to replace the zwitterionic detergent LDAO with the positively charged detergent cetyltrimethylammonium bromide (CTAB). To avoid precipitation, the CTAB was introduced to the samples that contained 0.03% DOC or TX-100 by simple mixing prior to the experiments. The final concentration of CTAB was maintained at 0.04%. Whether TX-100 or DOC was present with the CTAB had no influence on the spectra or the kinetics. Because of the extensive dialysis of the samples the secondary quinone activity was ∼10% as checked by flash-induced absorption changes measured with a miniaturized laser flash photolysis unit (LFP-112 from Luzchem Research Co., Ottawa, Ontario, Canada). Reconstitution of the RCs to unilamellar vesicles was prepared by the gel filtration, micelle-to-vesicle transition method.[36] The phospholipids were dissolved in chloroform and were purged with nitrogen stream to form a thin film on a surface of a conical tube. The film then was dissolved in 0.5 mL of 4% sodium cholate, 15 mM potassium phosphate, 15 mM KCl, pH 7.4. The dispersion was sonicated for 20−25 min to form clear phospholipid/detergent mixed micelles. After the addition of the RC in ∼2 μM final concentration the mixture was agitated with a vortex mixer to allow the phospholipid/protein/detergent mixed micelle formation. The dispersion was then loaded on a Sephadex G-50 superfine gel filtration column that had been previously equilibrated with 15 mM potassium phosphate, 15 mM KCl, 1 mM EDTA, pH 7.4. The fraction containing the liposomes with the incorporated RCs was collected. Finally, the liposomes were filtered through a 220 nm pore size filter (Millipore). The following lipids were used: 1,2-dioleoyl-*sn*-glycero-3-phosphocholine (DOPC), 1,2-dioleoyl-3-trimethylammonium−propane (DOTAP), 1,2-dioleoyl-*sn*-glycero-3-phospho-L-serine (DOPS), and 1,2-dilauroyl-*sn*-glycero-3-phosphocholine (DLPC). All lipids were purchased from Avanti Polar Lipids (Alabaster, AL) and were used without further purification.

All RC purification and handling steps were done in near darkness to ensure that the samples remained strictly in the dark-adapted states before the controlled illuminations during the recording of the spectra and kinetics.

Optical Spectroscopy. Optical spectra in the 700−1000 nm spectral range and kinetics of the absorbance changes induced by continuous illumination were measured using a Varian Cary 5000 spectrophotometer (Mulgrave, Victoria, Australia). The illumination was performed with a 250 W tungsten lamp (Oriel 6129, Newport Corp., Irvine, CA) connected to a fiber optics (Newport Corp.) that was oriented perpendicular to the monitoring beam. An interference filter with maximum transmittance at 850 or 870 nm was also mounted on the fiber optics. The light intensity was set to ∼30% of the saturating value at 1.5 μM RC concentration. The spectra were recorded at the maximum ∼1800 nm/min scanning rate. Kinetic traces were analyzed by decomposition into exponentials using the Marquardt nonlinear least-squares method. All measurements were performed at room temperature.

Spectroelectrochemical Redox Titrations. The oxidation−reduction midpoint potential of the P/P^+ couple was determined by spectroelectrochemical oxidation−reduction titrations both in the dark and under a weak continuous, external illumination as described previously.[28] The intensity of the illumination was poised to achieve the bleaching of ∼5% of the P-band. This use of weak illumination limited photodamage during the long experiments (∼2 h) and ensured that the vast majority of P was in its reduced state at any given time. The angle of the illumination was ∼45° with respect to the propagation of the monitoring beam to avoid stray light entering the detector chamber. The degree of the electrochemical oxidation of P was determined by monitoring the absorption at the maximum of the Q_y band centered at 865 nm in wild type from the near-infrared (700−1000 nm) spectra recorded at different ambient redox potentials with a Cary 5000 spectrophotometer. The ambient redox potential was adjusted with a CV-27 potentiostat from Bioanalytical Systems (West Lafayette, IN), and the reaction centers were placed into a thin-layer spectroelectrochemical cell of local design containing a 333 lines/in. gold mesh (Precision Eforming, Cortland, NY), based upon a cell design previously described.[28,37] A miniature calomel electrode (Cole Palmer, Vernon Hills, IL) was used as the reference electrode. The calibration of the calomel electrode potential was done according to O'Reilly.[38] Potassium hexacyanoferrate(II) and potassium tetracyanomono(1,10-phenanthroline)ferrate(II) were added as redox mediators. The data were fitted with the Nernst equation as described earlier.[28,35,37] The RCs for the electrochemical titrations were concentrated to ∼300 μM and were kept in 0.05% TX-100 or DOC depending on the experiment, 1 mM EDTA, 15 mM Tris-HCl, 70 mM KCl. All measurements were performed at room temperature.

RESULTS

Comparison of the Light-Minus-Dark Spectra and the Recovery Kinetics of the Dimer in Detergent Micelles. The absolute and light-minus-dark difference optical spectra were recorded during and various different times after the illumination for RCs from *Rba. capsulatus* that were dispersed in DOC, CTAB, and LDAO (Figure 1). The absolute spectra have three absorption bands in the 700−1000 nm region. The band centered at ∼760 nm is assigned to the H molecules (H-band), the second band centered at ∼800 to the B molecules (B-band), and the third at 850−870 nm to P (P-band). The near-infrared absolute absorption spectrum is significantly different if the RCs are dispersed in positively (CTAB) or negatively (DOC) charged detergent micelles as reported earlier. The most striking effect is a ∼20 nm blue shift in the position of the P-band, that is clearly visible in the absolute spectra. The difference spectrum (thick solid line in panel A) reveals an additional feature, namely a slight broadening of the B-band if the detergent is changed from DOC to CTAB. The band shift and broadening are two standard electrochromic responses to changes of the local electric field.[40] The light-minus-dark difference optical spectra measured at

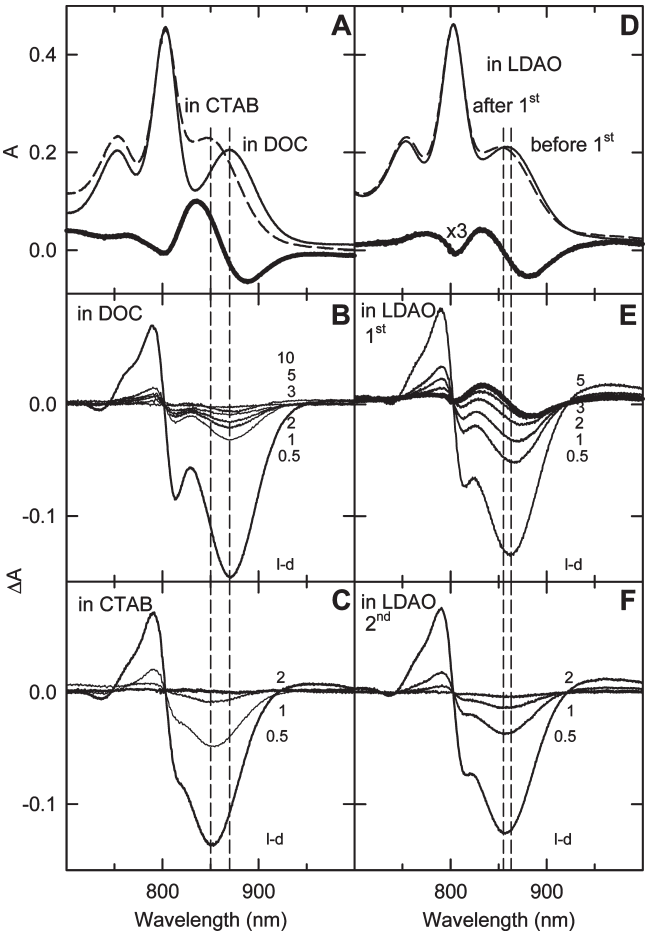

Figure 1. Near-infrared absolute (panels A and D) and light-minus-dark difference optical spectra (recorded at the end of 1 min illumination) and recovery in reaction centers dispersed in DOC (B), CTAB (C), and LDAO during and after the first (E) and second (F) illumination. The position of the P-band in these samples is indicated by vertical dashed lines. The numbers in the difference spectra in panels B, C, E, and F show what time the spectra were recorded in minutes after the illumination was turned off. In LDAO the position of the P band was found to be different before and after the first illumination. The thick solid lines in panels A, D, and E represent the difference spectra recorded in DOC and CTAB, before and after the first illumination in LDAO, and the residual spectra after the first illumination, respectively. These difference spectra are consistent with the shift of the P-band from 870 to 850 nm in panel A and from 863 to 855 nm in panels D and E, respectively. Conditions: 1.5 μM RC, 15 mM Tris-HCl, 1 mM EDTA pH 8. The concentrations of the detergents are listed in the text.

different times after illumination are shown for DOC and CTAB in panels B and C, respectively. In both detergents the difference spectra feature bleaching of the P-band, an electrochromic blue shift of the B-band due to the presence of the positive charge on the nearby P, and an electrochromic red shift of the H-band due to the negative charge on Q_A.[41] After illumination for 1 min, the spectra recovered fully but with different rates for RCs in CTAB and DOC. In CTAB total recovery was observed within 2 min after the illumination was switched off, while in DOC the full recovery required a ~4 times longer time scale. The spectra for DOC and CTAB samples were insensitive to the illumination history of the sample, meaning that subsequent illuminations resulted in the same spectra, but this was not the case for the LDAO-dispersed samples. Using strictly dark-adapted samples, the position of the P-band was 863 nm, a value very close to 865 nm that is observed in TX-100 for *Rba. capsulatus* or for *Rba. sphaeroides* in both TX-100 and LDAO. During the very first illumination, however, the position of the P-band shifted to 855 nm and did not return even after 1 h dark adaptation (panel D). The difference spectrum in LDAO between the spectra collected after and before the first illumination shows the very same features as those determined between CTAB and DOC (panel A). Panel E shows the lack of full recovery after the first illumination. Subsequent illuminations, however, did not cause further shifts as the spectral features recovered fully (panel F). A single illumination causes only a fraction of the RCs to be converted to a long-lived, conformationally altered state generating a heterogeneous population of the RCs. Using subsequent exposures, the position of the P-band eventually shifted to 850 nm after five 1 min long illuminations followed by 10 min dark relaxation periods after each exposure and stayed there even after several hours dark adaptation. One full day in the dark resulted in a few nm red shift in the P-band position, indicating that a very small fraction of P may have returned to the dark-adapted 865 nm position. Such long time storage at room temperature, however, began to take a toll on the stability of the RC protein as additional changes characteristic to degradation processes also appeared in the spectrum. It has to be noted that the recovery kinetics after the first illumination was slower than after the second illumination in LDAO, in the same manner as in DOC vs in CTAB (please compare panels B with E and panels C with F). If much longer (15 min) illumination was used even in DOC and TX-100, the light-induced shift to 850 nm could be induced and the partial recovery of the band position took several hours (data not shown).

Complex formation and recovery kinetics during and after illumination (Figure 2) indicates that the continuous illumination drives a fraction of the RCs to a conformationally altered state as described previously.[20−22,24,25,27,28] Under the applied conditions the charge-separated state was formed immediately. In addition to the unresolved, rapid absorption change, a further slower increase of the signal was also observed. The slow increase of the signal was interpreted to be arising from altered populations of the RCs generated by the continuous illumination. In the recovery kinetics similarly the fast, unresolved phase (in the minute scale) was interpreted to arise from the charge recombination in the fraction of the samples still in the dark-adapted conformation. This phase is assumed to have the same rate constant as that observed after single flash excitation. The second, much slower phase was assigned to the recovery of the charge-separated state in the fraction of the RCs that underwent light-induced structural changes near P.[27,28] Analysis of the slow

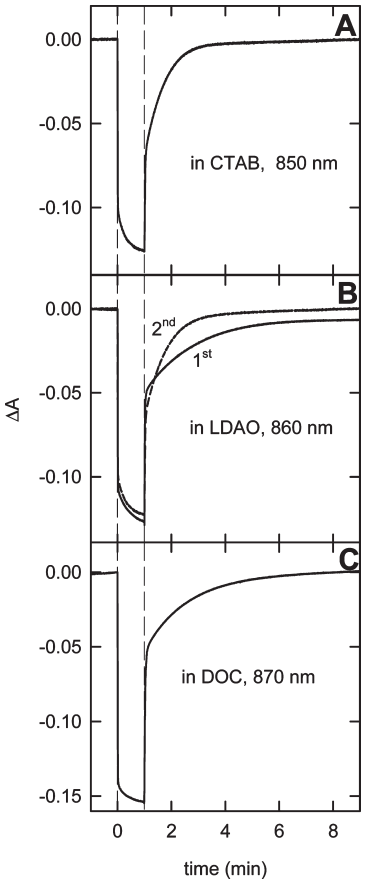

Figure 2. Kinetics of the light-induced absorption changes measured in the Q_y absorption band of P during and after 1 min illumination in the absence of any secondary donor for RCs in (A) CTAB, (B) LDAO, and (C) DOC. In LDAO the kinetics was dependent on whether the samples were dark-adapted or preilluminated. Vertical dashed lines indicate when the illumination was turned on and off. Note that the kinetic trace in LDAO after the first illumination does not recover completely to zero (see panel E in Figure 1 for comparison). Conditions as in Figure 1.

phase in the different detergents yielded rate constants of 9.8×10^{-3} and 2.4×10^{-2} s^{-1} in DOC and CTAB, respectively. A similar, ~2-fold difference was observed in LDAO when comparing the slow phases of the first and second illuminations, which had rate constants of 9.4×10^{-3} and 1.9×10^{-2} s^{-1}, respectively. The kinetic parameters are also listed in Table 1. These results indicate that the rate constants are essentially the same for RCs that have the long-wavelength form of P and similar for those that have the short-wavelength form of P regardless of the identity of the detergent. As the position of the P-band in *Rba. sphaeroides* can only be shifted to 850 nm with the addition of cationic detergent (CTAB),[30] the dependence of the recovery kinetics in the presence of CTAB was measured. A pronounced ~3-fold acceleration of the recovery was found for RCs from *Rba. sphaeroides*, with rate constants ranging from 9.4×10^{-3} to 3.0×10^{-2} s^{-1} as the band position moved from 865 to 850 nm upon addition of CTAB (data not shown).

The normalized light-minus-dark difference spectra measured at the beginning of the illumination and 1 min after the illumination was turned off in *Rba. capsulatus* in DOC, CTAB, and LDAO are shown in Figure 3. The spectra recorded at the beginning of the 1 min illumination are predominantly

Table 1. Kinetic Parameters of the Recovery of the $P^+Q_A^-$ Charge Pair after Continuous Illumination in RCs from *Rba. capsulatus*[a]

	headgroup charge[b]	name[c]	A_s[e]	$k_s \times 10^2$ (s^{-1})[f]	A_{vs}[e]	$k_{vs} \times 10^3$ (s^{-1})[f]
detergent	+1	CTAB C_{12}	0.53	2.4	ND	ND
	0	LDAO C_{12} 1st	0.41	0.94	ND	ND
		LDAO C_{12} 2nd	0.50	1.9	ND	ND
	−1	DOC[d] C_{22}	0.37	0.98	ND	ND
lipid	+1	DOTAP C_{18}	0.24	1.8	0.30	1.7
	0	DOPC C_{18}	0.22	2.0	0.32	2.5
		DLPC C_{12}	0.42	1.1	ND	ND
	−1	DOPS C_{18}	0.16	1.4	0.51	0.9

[a] The RCs were dispersed either in detergent micelles or in liposomes with various headgroup charges and the kinetic parameters were determined from Figures 2 and 8, respectively. ND: not detectable. [b] Net charge of the headgroup at pH 7.4. [c] Abbreviated name of the detergent or lipid and the length of the hydrophobic chain. [d] Effective length C_{12}−C_{13}. [e] Relative amplitude of the slow (A_s) and very slow (A_{vs}) components in the recovery of the $P^+Q_A^-$ charge pair. [f] Rate constant of the slow (k_s) and very slow (k_{vs}) components.

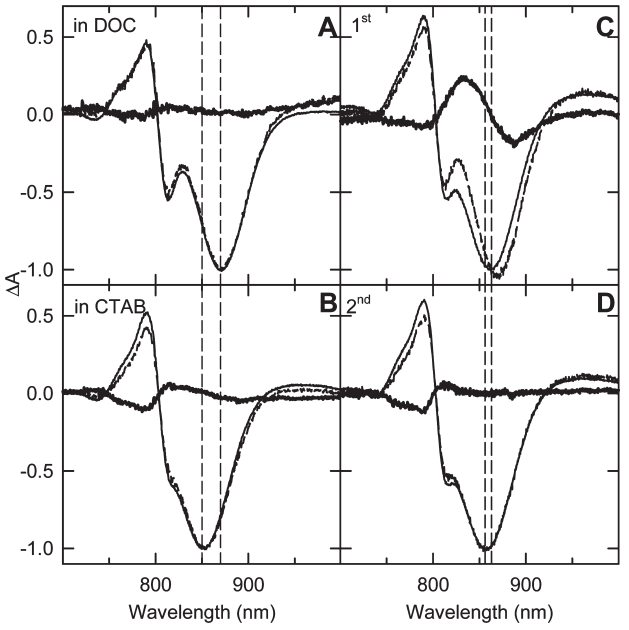

Figure 3. Normalized light-minus-dark difference spectra (solid lines) recorded immediately after the onset of the light and 1 min after the illumination was turned off (dashed lines) for RCs dispersed in DOC (A), CTAB (B), and LDAO (C and D, for the first (1st) and second (2nd) illuminations, respectively). The thick solid lines show the double difference spectra and feature changes around 800 nm consistent with the decrease of the electrochromic absorption changes involving the monomers during the illumination. The vertical dashed lines show the position of the P-band in DOC, CTAB, and in LDAO before and after the first illumination. Conditions as in Figure 1.

characteristic of the dark-adapted conformation of the RC, while those recorded 1 min after the illumination is turned off represent the light-induced conformation in all samples. The differences between those two spectra are characteristic of the light-induced changes that took place during illumination. A decrease of the electrochromic absorption changes of the B-bands was detected in *Rba. capsulatus* in all three detergents regardless of the position of the P-band, which is similar to the findings for RCs from *Rba. sphaeroides*.[27] However, in the strictly dark-adapted RCs in LDAO, the double difference spectrum featured not only the shift in the B-band but also the shift in the P-band (Figure 3C).

Reversible Shifts of the P-Band in the Presence of Secondary Donors. The possibility of inducing a shift of the P-band reversibly during illumination in RCs that were dispersed in LDAO was also investigated. For this purpose, a secondary electron donor, 2,3,5,6-tetramethyl-*p*-phenylenediamine (DAD), was added to strictly dark-adapted samples. After illumination, the secondary donor reduces P^+ and the measured spectra are characteristic only of the reduced quinone. Such spectra feature an electrochromic red shift of the H-band due to the negative charge on the nearby quinone and a much smaller electrochromic blue shift of the P-band.[42] The influence of the negative charge on the shift of the P-band is very small given the almost 3 times larger distance between Q_A and P compared to the distance between Q_A and H. The requirement for an efficient secondary electron donor is that the electron donation should be faster than the charge recombination as these two processes are parallel reactions. The electron donation time of various, routinely used secondary donors spans over 3 orders of magnitude in time. The native secondary donor, cytochrome c_2, donates an electron to P^+ in one or a few microseconds depending on whether it was already bound to the RC or it must diffuse to the binding site.[43] Ferrocene donates an electron to P^+ in ∼250 μs in RCs from *Rba. sphaeroides*.[44] DAD is the slowest among the routinely used secondary donors with a donation time of >1 ms.[45] This is still about 100-fold faster than the charge recombination and qualifies DAD as a sufficient secondary donor.

For strictly dark-adapted RCs after addition of DAD, the light-minus-dark difference spectrum has a pronounced electrochromic shift of the P-band that is strongly dependent upon pH (Figure 4A, solid lines). The amplitude of the electrochromic shift was very small at pH 6 and reached its maximum value at pH 8 with a slight decrease at higher pH values (Figure 4B, closed symbols). This electrochromic shift corresponds to the shift of the P band from 863 to 855 nm in a varying fraction of the RCs. Once the spectral features fully recovered several minutes after illumination, subsequent illuminations resulted in almost the same spectra with slightly smaller amplitudes of the electrochromic shifts on the P-band but without any decrease of the electrochromic shift of the H-band. However, if the RCs were pre-exposed to illumination prior to the addition of DAD, the large electrochromic shift of the P-band was completely missing and the pronounced pH dependence was also lost (Figure 4A, dashed lines; Figure 4B, open symbols). Preillumination on the

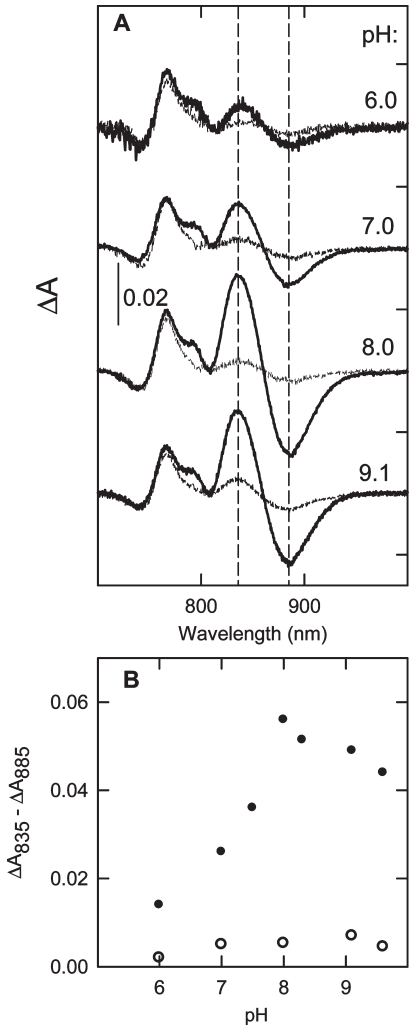

Figure 4. (A) Light-minus-dark difference optical spectra of the RCs in the presence of a secondary donor (DAD) in the dark-adapted (thick solid lines) and preilluminated samples (thin solid lines) at the pH values of 6.0, 7.0, 8.0, and 9.1. In the preilluminated samples the DAD was added after 10 min dark adaptation. Conditions as in Figure 1 except +500 μM DAD. (B) pH dependence of the peak-to-trough difference of the shift of the P-band measured at 885 and 835 nm in dark-adapted (closed symbols) and preilluminated samples (open symbols).

other hand did not influence the electrochromic shifts of the H-band (Figure 4A).

After illumination, the electrochromic shift of the P-band recovered with biphasic recovery kinetics (Figure 5). Kinetic traces were recorded at the maximum values of the spectral changes, namely at 885 and 835 nm (Figure 4). For both wavelengths, the recovery had a dominant amplitude (87−88%) with a rate constant of $(1.2-1.4) \times 10^{-1}$ s^{-1} with the remaining 12−13% component having a rate constant of $(1.1-1.5) \times 10^{-3}$ s^{-1}. In the preilluminated samples the rate constants were similar but the relative amplitudes differed as 75% recovered with a rate constant of $\sim 10^{-1}$ s^{-1} and 25% with a rate constant of $\sim 10^{-3}$ s^{-1}. Using cytochrome *c* as a secondary donor, the large electrochromic shift of the P-band was not observed, and the recorded spectra were similar to those obtained for the preilluminated samples (data not shown). It is not clear whether this is due to electrostatic interactions associated with the docking of the cytochrome or the nearly 3

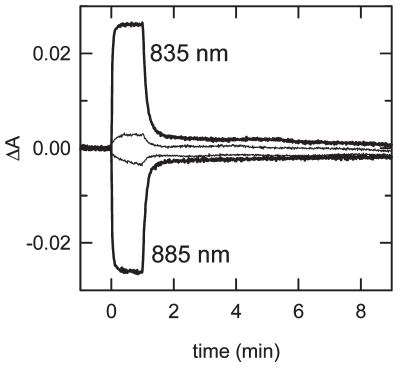

Figure 5. Kinetics of the light-induced absorption changes in the presence of DAD as a secondary electron donor in dark-adapted (thick solid lines) and in preilluminated (thin solid lines) RCs. The traces were measured at the maximum values (885 and 835 nm, see Figure 4) of the spectral signatures associated with the blue shift of the P-band. Conditions as in Figure 4.

orders of magnitude faster electron donation time for cytochrome *c* compared to DAD. Using ferrocene, which also donates an electron in a second order process like DAD, intermediate size electrochromic shifts were observed in the P-band, indicating that P^+ should be present for at least a submillisecond time scale to build up the large electrochromic shifts. It should also be mentioned that in the presence of terbutryne, an inhibitor of electron transfer to Q_B, the large electrochromic shifts are not observed, even in dark-adapted samples, but in the presence of a different inhibitor, stigmatellin, the shifts were observed (data not shown).

Potential of the P/P$^+$ Couple in the Light-Induced States. The P/P^+ oxidation/reduction midpoint potential was measured for RCs from *Rba. capsulatus* in TX-100 and DOC using spectro-electrochemical titrations (Figure 6). Without any external illumination the data were well described using the Nernst equation assuming only one population of P, yielding midpoint potentials (E_m) of 500 and 480 mV in TX-100 and DOC, respectively. Under these conditions, the peak position of the P-band was at 865 and 870 nm for TX-100 and DOC, respectively (Figure 1). The error is estimated to be ±5 mV based upon the results obtained from different titrations in the dark.

The midpoint potentials were also measured while the samples were weakly illuminated according to the method introduced earlier.[28] The dependence of the fraction reduced on the potential required the use of a two-component Nernst equation assuming two populations of P with different E_m values as previously found for RCs from *Rba. sphaeroides*.[28] One population represents the RCs that are in the dark-adapted conformation, and another fraction is characteristic of the light-adapted conformation. While the potentials of the fractions with an unchanged P-band position did not change, those with blue-shifted P-band positions exhibited much lower P/P^+ potentials with values of 340 and 360 mV in TX-100 and DOC, respectively. These decreases of the E_m value in RCs from *Rba. capsulatus* are about twice as large as the values of the decreases reported in *Rba. sphaeroides* where the P-band position remained at 865 nm even in the light-adapted conformation.[28] Unlike in *Rba. sphaeroides*, prolonged illumination of RCs from *Rba. capsulatus* results in the position of the P-band shifting in one fraction of the RCs to 850 nm in TX-100 and DOC in addition to the decrease of the electrochromic shifts of the B-bands (see insets in Figure 6). The spectroelectrochemical redox

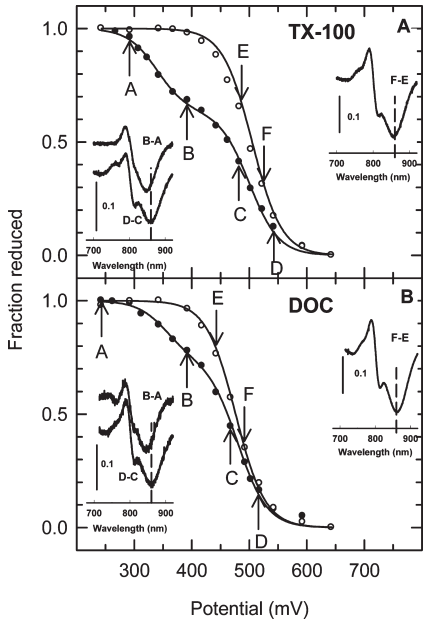

Figure 6. Spectroelectrochemical redox titrations of the RCs in the absence (open symbols) and in the presence (closed symbols) of a weak external illumination in TX-100 and DOC. The data were fitted with a standard Nernst equation assuming one (in the dark) or two (in the presence of illumination) components. The fit yielded the following values for the P/P^+ potentials: TX-100: 500 mV (100%) in the dark and 500 mV (60%) and 340 mV (40%) in the presence of illumination; in DOC: 480 mV (100%) in the dark and 480 mV (75%) and 360 mV (25%) in the presence of illumination. The inserts show the difference spectra between two absolute spectra recorded at two different applied potentials in the appropriate range indicated by the arrows and letters from A to F. The vertical dashed lines in the insets are drawn at 865 nm. Note the shifted P-band positions and the decreased electrochromic shifts in the spectra of the light-induced conformations. Conditions ~300 μM RC, 70 mM KCl, 1 mM EDTA, 0.05% TX-100 or 0.05% DOC.

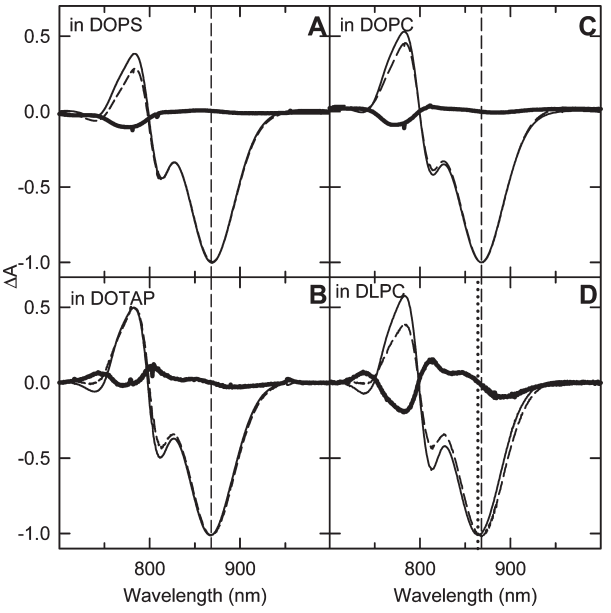

Figure 7. Normalized light-minus-dark difference spectra (solid lines) recorded immediately after the onset of the light and 1 min after the illumination was turned off (dashed lines) for RCs from *Rba. capsulatus* incorporated in DOPS (A), DOTAP (B), DOPC (C), and DLPC (D) liposomes. The thick solid lines show the double difference spectra and feature changes around 800 nm, consistent with the decrease of the electrochromic absorption changes involving the monomers during the illumination and in DLPC a marked shift in the P-band. The vertical dashed lines show the position of the P-band in DOPS, DOTAP, and DOPC at 868 nm. The vertical dotted line is indicating the position of the P-band in DLPC at 864 nm. Conditions: ~1.5 μM RC, 15 mM potassium phosphate, 15 mM KCl, 1 mM EDTA, 100 μM terbutryne, pH 7.4.

titrations could not be performed for RCs in LDAO due to an undetermined but earlier reported interaction between the LDAO and the electrodes.[39] Also, measurements could not be performed in CTAB due to instability of the samples.

Influence of the Lipids on the Light-Induced Optical Spectra and the Kinetics of the Recovery of the Charge Pair in Liposomes. Light-minus-dark optical difference spectra were recorded both in chromatophores (data not shown) and in RCs from *Rba. capsulatus* that were reconstituted into liposomes. The liposomes were formed using lipids that all contained the same monounsaturated dioleoyl (18 carbon atoms long, C_{18}) fatty acid chain but with different headgroups, positive (DOTAP), negative (DOPS), or zwitterionic (DOPC) (Figure 7). This selection ensured that all three lipids were in their liquid crystalline phase at room temperature with only differences in their headgroup charges. Following the same approach shown in Figure 3 for detergent micelles, the normalized spectra taken at the beginning of the illumination (solid lines) and 1 min after the illumination was turned off (dashed lines) are shown in Figure 7 for the liposomes. For comparison, the spectra recorded in RCs that were incorporated to liposomes from DLPC with zwitterionic headgroups like DOPC but only a C_{12} fatty acid chain are also shown (Figure 7D). Unlike for the spectra recorded in detergent micelles (Figure 3), the headgroup charges had no significant influence on the peak position of the P band as long as the fatty acid chains were C_{18}. All RCs exhibited P band positions of 868 ± 1 nm in the dark (data not shown) and at the beginning of the illumination (vertical dashed lines in Figure 7, panels A−C). The prolonged illumination of these RCs did not change the position of this band significantly as indicated by the lack of spectral features in the double difference spectra (thick solid lines) in the 840−900 nm range. If, however, the RCs were reconstituted into liposomes from DLPC with a zwitterionic headgroup and a C_{12} fatty acid chain, the observed position of the P-band at the beginning of the illumination (and in the dark prior to illumination) was already blue-shifted by 4 nm to 864 nm. Upon illumination the observed P band position shifted even further to lower wavelengths, though not as much as observed for RCs in zwitterionic LDAO detergent micelles (Figure 3C). Analysis of the double difference spectrum (thick solid line in Figure 7D) showed a shift of the P-band to 850 nm in 27% of the RCs. The observed very small, light-induced shift in DOTAP indicated only 7% of the RCs as being affected (Figure 7B). Unlike RCs in LDAO, the peak position of the P-band during the recovery returned to the value observed before the illumination both in DOTAP and in DLPC liposomes. The spectra recorded after the illumination was turned off were characteristic of the $P^+Q_A^-$ state in the light-adapted conformation and showed decreased electrochromic shifts of the B-bands around 800 nm. The decreases of the electrochromic absorption changes involving the B bands around 800 nm upon illumination were present

in all samples but with different extent (Figure7). The recovery kinetics of the $P^+Q_A^-$ charge pair after illumination is shown in Figure 8, and the kinetic parameters are tabulated in Table 1 for RCs incorporated into liposomes. The time required for the full recovery of the charge-separated state was found to be much longer in liposomes with C_{18} fatty acid chains (DOTAP, DOPC, and DOPS) than in DLPC liposomes with C_{12} fatty acid chain length. In DLPC liposomes and detergent micelles, the recovery kinetics were biphasic with the slow component being comparable in all detergent micelles and lipids (see also Figure 2 and Table 1). In liposomes with the lipids with C_{18} fatty acid chains, the recovery kinetics had a third, very slow component. This very slow component had nearly an order of magnitude smaller rate constant than that of the slow component (Table 1).

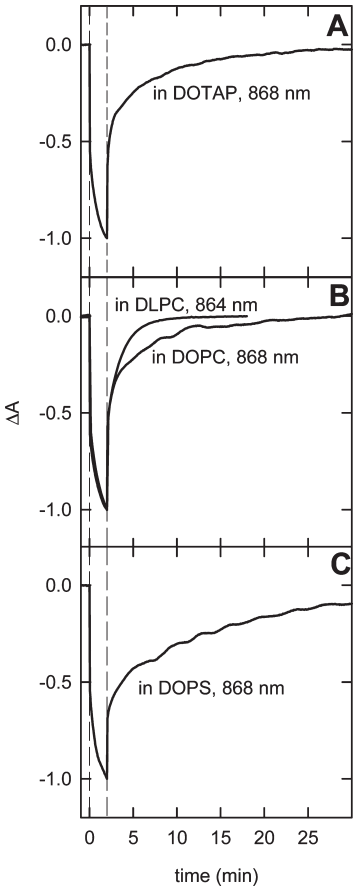

Figure 8. Kinetics of the light-induced absorption changes measured in the Q_y absorption band of P during and after 2 min illumination in the absence of any secondary donor for RCs in liposomes with different headgroup charges: (A) DOTAP (positive), (B) DOPC and DLPC (zwitterionic), and (C) DOPS (negative). Vertical dashed lines indicate when the illumination was turned on and off. Conditions as in Figure 7.

DISCUSSION

Light-induced hypsochromic shifts of the Q_y absorption band of P in RCs from *Rba. capsulatus* were observed that are modeled as being associated with light-induced conformational changes near P. These optical shifts were only visible in dark-adapted samples of RCs in zwitterionic LDAO that had not been previously exposed to light and in liposomes formed from also zwitterionic DLPC lipids but with short (C_{12}) hydrophobic fatty acid chains. In the absence of a secondary electron donor, these shifts appeared to be irreversible in LDAO but not in DLPC, while in the presence of DAD, which serves as a secondary electron donor to P^+, the shifts could (nearly) reversibly be reproduced. Associated with the shift is a 2-fold increase of the rate constants for the recovery of the charge-separated state after prolonged illumination in LDAO detergent. Similar results were obtained when the detergent was changed from the negatively charged detergent DOC to the positively charged detergent CTAB. In liposomes the shift from a long-wavelength to a short-wavelength form resulted in a more dramatic change in the recovery kinetics (Figure 8 and Table 1). The P/P^+ potential and electrochromic absorption changes of the B-bands during illumination were also dependent upon the choice of detergent. Similar features were observed in RCs from *Rba. sphaeroides* and interpreted as arising from conformational changes near P.[27,28] The influence of the headgroup charge and the hydrophobic thickness of the membrane substituent on the light-induced structural changes and on the electronic structure of P are discussed.

Two Distinct Conformations of P. On the basis of their spectral features, the RCs can be divided into two classes depending on the observed position of the Q_y absorption band of P, with the band being at 865 and ~850 nm for the first and second classes, respectively.[29] Under the most commonly used RC purification conditions, RCs from *Rba. sphaeroides* and

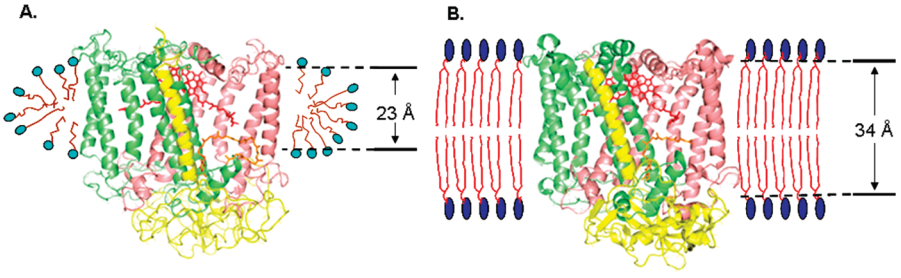

Figure 9. Schematic ribbon representation of the bacterial reaction center in a LDAO detergent micelle (A) and in a lipid bilayer with oleoyl fatty acid chains (B). The L, M, and H subunits are labeled with salmon, lime, and yellow colors, respectively. The bacteriochlorophyll dimer (P) and the primary quinone (Q_A) are also shown as red and orange sticks, respectively. The differences in the hydrophobic thicknesses between the RC and the lipid bilayer or detergent belt are shown, and this difference is proposed to alter the electronic structure of P and thus shift the position of the P-band. The coordinates for the RCs were taken from PDB entry codes 1YST (A) and 1OGV (B).[66,72] The lipids and detergents are not shown as precise molecular structures but rather drawn only as schematic representations. The hydrophobic thicknesses of the detergent belt and the lipid bilayer were taken from refs 65 and 72, respectively.

Rhodospirillum (Rps.) rubrum belong to the first class and *Rba. capsulatus* and *Rps. centenum* were reported to belong to the second group. For RCs from both *Rba. capsulatus* and *Rba. sphaeroides*, it is possible to shift the P-band position and thus convert one spectral form of P to another by changing the nature of the detergent.[29,30] Positively charged detergents like CTAB fix the position of the P-band at ~850 nm while neutral or negatively charged ones adjust the band position to ~865 nm. Contrarily to the behavior in LDAO the P-band position for RCs from both species in chromatophores is reported as 865 nm.[29] Our results showed that in liposomes formed from lipids with C_{18} fatty acid chains the P-band position was also preserved at the long-wavelength form (Figure 7). Our results also indicate that illumination can shift the P-band from its long-wavelength form to its short-wavelength form regardless of the identity of the detergent and also in liposomes from DLPC with short fatty acid chain length. The quantum yield of this conversion is reasonably high in LDAO but low in TX-100 and DOC as indicated by the differences in illumination times that are required to induce the shift (Figure 2). The conversion of the two spectral forms back and forth indicates that the spectral differences must be due to altered interactions of P with the environment and not due to inherent structural differences. The major difference between these two forms is the ability to delocalize the positive charge over the two halves of P. Extensive electron paramagnetic resonance (EPR) and electron nuclear triple resonance (special TRIPLE) studies have revealed that the observation of the long-wavelength form is coupled to a larger degree of delocalization of the positive charge (electron hole) with a ratio of approximately 2:1 favoring P_L over P_M.[46] Contrarily, the positive charge is almost completely localized on P_L if the band position is found at 850 nm setting the same ratio to 5:1. The observed asymmetry was attributed to the change in the orbital energies of the two halves of the dimer.[47] The change in the delocalization of the positive charge and thus the orbital energies was proposed to be caused by a change of the orientation of the 2-acetyl groups of P_L and/or P_M.[30,46,48,49] These studies indicated that 2-acetyl groups have different orientations when they are free or hydrogen-bonded to nearby residues. Whether or not the rotation of the 2-acetyl group causes the shifts in the P-band position and in the spin density distribution between P_L and P_M is not clear. Removal of the native H-bond in *Rba. sphaeroides* between the 2-acetyl group of P_L and the L168 His by substituting this residue with a Phe resulted in the shift of the P-band to 850 nm, but the electron hole became almost evenly shared between the two halves of P instead of the predicted localization on P_L.[48] This is in contrast to what was observed in native RCs dispersed in positively charged detergents, where the 850 nm P-band position was coupled to an almost total localization of the hole on P_L.[30] Similarly, if H-bonds were introduced in the symmetrical position between the 2-acetyl group of P_M and a residue substituted to the M197 position depending on the identity of the residue different results were obtained. The formation of the H-bond was confirmed with both His and Tyr residues with various techniques.[48−50] With His at M197 significant changes could be observed neither in the spin density distribution nor in the position of the P-band in comparison with wild type.[39,48] With Tyr at M197, however, both the blue shift of the P-band and the localization of the hole on P_L were observed.[50] The picture becomes even more complicated if we compare the changes of the reported P/P^+ potentials caused by the removal or addition of the H-bonds and thus the rotation of the corresponding acetyl groups. The M197 His induced the largest increase of the P/P^+ potential (130 mV) regardless of the lack of the spectral changes, while the Tyr only increased the potential by 30 mV.[39,51] In the symmetrical position, L168, the replacement of His with Phe resulted in a 90 mV decrease in the potential of P.[39] Some of the discrepancies can be explained since the P/P^+ potentials are not relevant if determined in dark-adapted samples as they are significantly different in the light-induced conformations under continuous illuminations (Figure 5).[28] Nearly all spectroscopic (other than optical) analyses of P^+ (ENDOR, FT-Raman, FTIR, EPR) were done in detergent dispersed RCs that were illuminated with continuous light.[30,46,49,52,53]

The orientations of the acetyl groups are proposed to influence the position of the P-band and the potential of P in the light-adapted conformation (Figure 6). Previously, the rotation of the acetyl group during light-induced conformational changes had been proposed in *Rba. sphaeroides*, but a shift of the P band was not observed for those RCs.[27,28] It appears that only certain orientations cause the shift of the P-band. The possible influence of different orientations of the 2-acetyl groups of P_L in RCs from different organisms on the P-band position is supported by FT Raman investigations as the vibrational frequencies of the H-bonded acetyl groups of P_L show small but significant variations when comparing *Rba. sphaeroides* and *Rba. capsulatus*.[52] A similar two-state conformational model was proposed for a mutant RC from *Rba. capsulatus* for which amino acid residues M205 to M210 were replaced with the corresponding L subunit residues.[12] In this mutant the shift of the P-band was even more pronounced, from 853 to 820 nm, and the potential of the P/P^+ couple (in the dark) increased by ~50 mV. Similar changes were observed in a mutant of *Rba. sphaeroides* containing the replacement of Tyr M210 with Trp.[54] In *Rba. sphaeroides* the phenol group of Tyr M210 is within H-bonding distance to the 2-acetyl group of P_M and its possible involvement in the conformational change was proposed as a potential source for the light-induced rotation of the 2-acetyl group of P_M.[2,6,28,55] The residue Tyr M210 is conserved in *Rba. capsulatus* and is likely to be at a comparable distance to the 2-acetyl group of P_M. Two amino acid residues near P, Phe M208, which is ~3 Å away from Tyr M210, and Val M192, which is ~10 Å from P, are Ala and Asp in RCs from *Rba. capsulatus*.[6] Given the closeness of Phe M208 to Tyr M210, the difference between Phe and Ala might influence the rotational freedom of the 2-acetyl group of P. The light-induced decrease of the P/P^+ potential was measured to range from 55 to 79 mV in *Rba. sphaeroides* depending upon the pH,[28] while in *Rba. capsulatus* the decrease was twice as large at pH 8 (Figure 6) as discussed below.

Donor−Acceptor Interactions. In the presence of a secondary electron donor the Q_A^-/Q_A difference spectrum can be detected during the illumination.[42] A small electrochromic shift of the P band has been routinely observed in RCs from both *Rba. capsulatus* and *Rba. sphaeroides* and modeled as arising due to a long-range (28 Å) electrostatic interaction between these two cofactors.[42] The large electrochromic shifts reported here (Figure 5) have not been observed before. The question arises as to whether these large electrochromic shifts in the P-band are due to strengthened interactions with the quinone during illumination in dark-adapted LDAO-dispersed RCs. There have been several reports in the literature that suggest stronger interactions between the periplasmic and the cytoplasmic side of the RCs in *Rba. capsulatus* than in *Rba. sphaeroides*. In wild type RCs from *Rba. capsulatus* and the R-26 strain of *Rba. sphaeroides*,

fractional proton uptake and release upon charge separation has been observed and associated with changes in the pK_a values of the nearby protonatable side chains due to the transient charges on Q_A and P, respectively.[17,18] Amino acid replacements near Q_A at the M246 and M247 positions in RCs from *Rba. capsulatus* resulted in changes not only in the flash induced proton uptake but also in the proton release.[19] The larger proton release in these mutants was interpreted as being due to a long-range electrostatic interaction between the Q_A binding site and residues near the periplasmic side. The light-induced conformational switch from the long-wavelength form to the short-wavelength form of P was blocked by terbutryne in our experiments but was allowed with the use of stigmatellin even though there was only about 10% Q_B activity in our samples. The addition of these inhibitors did not prevent the formation of the long-lived charge-separated state and the decreased electrochromic changes in the B-bands during illumination but altered the lifetime of the light-induced state by about a factor of 2 (Figure 2). In chromatophores of *Rba. capsulatus*, the binding of various inhibitors that block the electron transfer between Q_A^- and Q_B have been reported to alter the redox potential of P by as much as ~50 mV depending on the redox state of Q_A and the identity of the inhibitor.[56] This suggests that only one element of the conformational change was turned on and off by the inhibitors, by the preillumination of the samples, or by the selection of the detergent.

The effect of the presence or absence of Q_B on the light-induced conformational changes in *Rba. sphaeroides* is not clear. One group has found no difference,[22] another reported significant differences whether Q_B was present or not,[24] while a third group found only differences at high pH values.[21] These groups used different detergents to disperse the RCs and also different inhibitors to block the electron transfer to Q_B. Terbutryne and stigmatellin were reported to bind to slightly different positions in the Q_B binding pocket.[57−59] Without any inhibitor the Q_B binding pocket can either be empty or occupied by a distal or a proximal Q_B. In our case without the inhibitors the site has only ~10% Q_B occupancy. When stigmatellin is added, it binds to the proximal position whereas terbutryne binds to a more distal position. Since the observed shifts in the P-band were only seen in dark-adapted samples if this shift is coupled to donor−acceptor interactions, it is most likely disrupted by terbutryne that occupies the place of the dark-adapted quinone and thus prevents the switch to a conformation that would move the quinone to the proximal position. A coupling between the shift of the 2-acetyl group(s) of P and the distal to proximal repositioning of Q_B upon illumination of the dark-adapted samples is supported by our results. Kinetically resolved electrochromic and electrogenic measurements associated with the reduction of the quinones demonstrated the mobility of this region of the protein.[60−62] These structural changes happen even if Q_B is not present and were associated with the structural changes that eventually facilitate the electron transfer between the quinones. The kinetics of these changes were reported to be in the hundreds of microseconds time scale, a good match to the kinetic limit for the shift of the P-band observed in the present study with the use of different secondary donors with a wide range of donation times. One might assume that the difference in the hydrophobicity of the applied secondary electron donors could also have some influence on the local electrostatics and thus on the shift of the P-band. Both DAD and ferrocene are neutral and sparingly soluble in water and can be expected to partition into a non-aqueous environment within the RC−detergent complex. Upon oxidation they could create a local cation analogous to the CTAB headgroup effect. The use of the water-soluble cytochrome *c* should not have this effect. Unlike in *Rba. capsulatus* the use of the same external electron donors in RCs from *Rba. sphaeroides* did not result in large shifts of the P-band.[42] Similarly, regardless of the headgroup charge no large shifts were observed when the RCs from *Rba. capsulatus* were incorporated to liposomes in the presence of secondary donors (data not shown). Thus, we assume that the local electrostatic interactions with the oxidized forms of the secondary donors do not contribute to the large spectral features observed in LDAO.

The pH dependence of the electrochromic shifts (Figure 4b) complements the pH dependence of the proton release reported for RCs from *Rba. sphaeroides* upon continuous illumination.[21,27,28] At pH 6, where a large proton release was observed, a negligible shift of the P-band was detected (or more precisely, the shift was observed only in a very small fraction of the RCs). At pH 8, where the proton release is reported to be the smallest the electrochromic signals associated with the shift of the P-band were the largest (Figure 4). This indicates that the effect arises from the combination of various electrostatic interactions that participate in the solvation of the charges.

Recovery Rates of the Redox States after Prolonged Illumination. In *Rba. sphaeroides*, where the position of the P-band in LDAO is 865 nm, the rate constant for the slow component in the recovery kinetics after prolonged illumination without a secondary electron donor was reported to be ~2×10^{-2} s^{-1}.[27] This value is in agreement with the rate constants observed for RCs from *Rba. capsulatus* dispersed in DOC and LDAO if the samples were dark-adapted. Upon the light- or detergent-induced shift of the P-band to 850 nm a ~2-fold acceleration was observed (Figure 2 and Table 1). The slow phase is assigned to the fraction of the RCs that undergo a light-induced conformational change. The amplitudes of the slow phase are comparable (30−50%) in the two species and those found in different detergents in *Rba. capsulatus* (Figure 2). The acceleration of the recovery kinetics was also detected in *Rba. sphaeroides* if the P-band position was induced to be blue-shifted by the addition of CTAB (data not shown). These observations suggest a close correlation between the lifetime of the charge-separated state in the light-induced conformation and the position of the P-band and thus the electronic structure of P. The light-induced shift of the P-band in *Rba. capsulatus* appears to be a consequence of conformational changes in the RC, but the recovery rates change by a factor of 2 compared to a 1000-fold difference between the recovery kinetics in the dark- and light-adapted conformations (Figure 3). When RCs from *Rba. capsulatus* were reconstituted into liposomes, the rate constants of the slow component were also found to be similar to those determined in detergent micelles, but further stabilization of the $P^+Q_A^-$ charge pair was observed in liposomes from lipids with C_{18} fatty acid chains regardless of the headgroup charge (Figure 8). This stabilization was characterized by the presence of the very slow kinetic component that has a rate constant of ~10^{-3} s^{-1} (Table 1). When this component was detected the P-band stayed in its long-wavelength form during illumination (Table 1 and Figure 7A−C). Contrarily, if DLPC with a C_{12} fatty acid chain length was used to incorporate the RCs, the very slow component was not observed and the P-band position has been blue-shifted (Figure 7D, Table 1, and Figure 8). The very slow component with a rate constant of ~10^{-3} s^{-1} was assigned recently in RCs from *Rba. sphaeroides* to a stabilization of the

conformationally altered state by proton release.[28] In the proton release Tyr M210 plays a critical role as it is situated within H-bond distance from the 2-acetyl group of P_M as discussed above. The lack of the very slow component in the recovery kinetics of RCs reconstituted into DLPC with a blue-shifted P-band is consistent with the rotation of the 2-acetyl group and the loss of the proton pathway between Tyr M210 and the solvent. In the presence of the secondary electron donor (DAD) the major kinetic component of the recovery associated with the shift of the P-band has a very similar rate constant ($\sim 10^{-1}$ s^{-1}) that was assigned to the recovery of P^+ in RCs with conformational changes only near the quinones due to the use of short light exposure (Figure 5).[27,28] In mutants of RCs from *Rba. sphaeroides*, where the conformational changes were blocked near P due to the presence of the H-bond between the 9-keto carbonyl group of P_L and the introduced His residue at the L131 position, the rate constant of the recovery after prolonged illumination was also $\sim 10^{-1}$ s^{-1}.

P/P$^+$ Potential. The 500 mV E_m value from RCs from *Rba. capsulatus* without external illumination is, within error, the same as the E_m value of 505 mV determined for *Rba. sphaeroides* under the same conditions.[39] The slight decrease of 20 mV in the potential for RCs in DOC is attributed to an electrostatic stabilization of P^+ by the negatively charged detergent headgroups compared to the neutral headgroups in TX-100. Such electrostatic stabilization of P^+ can be observed in TX-100 at higher pH values where many amino acid side chains become deprotonated.[17,63] The decrease of the P/P^+ potential in the light-adapted conformation was ~120−160 mV in RCs from *Rba. capsulatus* depending on the detergent, where the position of the P-band in this population was found centered at 850 nm (Figure 6). In RCs from *Rba. sphaeroides*, where the P-band position remained at 865 nm even in the light-induced conformation, the decrease of the potential was only 75 mV under the same conditions.[28] Since the dark-adapted conformations resulted in very similar potentials for the two species with the P-band position at ~865 nm, we conclude that the differences in the potentials in the light-adapted conformations are associated with the shift in the P-band position from 865−870 to 850 nm and arising from different orientations of the acetyl groups of P. Even though the decrease of the potential in the light-adapted conformation in TX-100 is about twice as large if the band position is shifted to 850 nm than if it remains at 865 nm after 1 min illumination, the trend in the recovery rates was found to be the opposite. The rate constants were found to be about twice as large in RCs with P-band position at 850 nm than in those with the P-band at 865 nm, indicating that the recovery from the light-induced conformation is not electron transfer limited.

Influence of the Hydrophobic Mismatch on the Position of the Dimer and on the Light-Induced Conformational Changes. The position of the Q_y band of P in the light-minus-dark spectra showed a different sensitivity to the headgroup charge when the RCs were in detergent micelles (Figure 3) compared to liposomes (Figure 7). For RCs dispersed in detergent micelles, the charge of the headgroup induced a shift in the P-band position not only in RCs from *Rba. capsulatus* but also in *Rba. sphaeroides*, converting one spectral form of P to another (Figure 3).[29,30] The shift was primarily induced by a positively charged (both in *Rba. capsulatus* and in *Rba. sphaeroides*) or zwitterionic (*Rba. capsulatus* only) detergent. Interestingly, this shift was not detected in RCs from *Rba. capsulatus* that were reconstituted into liposomes with various headgroup charges provided the monounsaturated fatty acid chain length was C_{18} for which P was in its long-wavelength form as also found in the natural membranes (Figure 7A−C). Contrarily to the findings in detergents, exposing these RCs to light did not shift the position of the P band in the zwitterionic DOPC (Figures 3C and 7C). It was reported earlier that various negatively charged membrane lipids in *Rba. sphaeroides* do not alter the position of the P band if the fatty acid chain lengths are C_{16} or C_{18}.[64] Therefore, it was not expected that the spectrum recorded in the negatively charged DOPS would show any shift in the dimer position, and it is in agreement with the observation obtained in the negatively charged detergent, DOC (Figures 3A and 7A). In DOTAP liposomes only a tiny fraction (7%) of the RCs experienced the light-induced hypsochromic shift. However, if we used a shorter lipid (DLPC) with a zwitterionic headgroup, a 4 nm blue shift of the P-band was observed even in the dark, which was shifted even further upon prolonged illumination corresponding to 27% of P being converted to its short-wavelength form upon illumination (Figure 7D). This fraction is in a reasonable agreement with the amplitude of the long-lived component in the recovery kinetics (Figure 7). All other spectral and kinetic features of the light-induced structural changes near P were present in all liposomes, namely the decrease of the electrochromic absorption changes of the B bands and the long-lived charge-separated state. On the basis of neutron diffraction studies of detergent-grown RC crystals, the thickness of the detergent belt for LDAO and β-octyl-glucoside micelles is only ~23 Å, whereas the thickness of the detergent phase along the transmembrane α-helices of the L and M subunits is ~30 Å (Figure 9A).[65,66] This difference provides a significant hydrophobic mismatch, which should be compensated for not only by the detergent but also by the protein.[67] In the natural membrane environment, from an energetics point of view, it is expected that the hydrophobic thickness are matched; however, there are examples that do not match.[68] For example, in eukaryotic cells the plasma membrane is thicker than the membranes of the endoplasmic reticulum; nonetheless, the proteins found in the plasma membrane are initially integrated in the endoplasmic reticulum.[68] Furthermore, the composition of the natural membrane is not unique in different photosynthetic bacteria.[69] Even within the same strain, for example changes in growth conditions can alter the membrane composition in *Rba. sphaeroides*.[70] Among the natural lipids the monounsaturated phospholipids are very common in the natural membrane and the thickness of the dioleoyl (C_{18}) fatty acid chain was calculated to be also 30 Å, the same as the length of the α-helices reported in *Rba. sphaeroides*.[65,71] The hydrophobic thickness of the DLPC bilayer in its liquid crystalline and gel phases was reported to be only 19.5 and 27.0 Å, respectively.[71] It is expected that in part of the compensation for the hydrophobic mismatch the phase transition temperature of saturated DLPC at the interface is shifted from ~0 °C toward room temperature values. Even if the shift is dramatic, it still cannot match the ~30 Å thickness of the hydrophobic length of the transmembrane helices. It was suggested that membrane proteins can compensate for the hydrophobic mismatch by tilting their transmembrane α-helices to reduce their effective thickness or adjust their hydrophobic length by changing the orientation of both the hydrophobic and hydrophilic side chains near the interface.[68] Recently, the crystal structure of *Rba. sphaeroides* was resolved in a lipidic cubic phase using also monounsaturated oleoyl lipids with C_{18} fatty acid chain lengths.[72] Comparison with eight detergent-based

structures revealed that the 2-fold symmetry axis passing through P and the nonheme Fe^{2+} is slightly tilted relative to the plane of the membrane, and the crystal contacts were structurally perturbed in the various structures by interactions with the surrounding detergent and lipid molecules. The crystal contacts along the symmetry axis were reported to be mediated by interactions between the periplasmic regions of the L and M subunits not far from P. In the lipid-based structure the membrane was clearly identifiable with a hydrophobic thickness of 34 Å, which is in a reasonable agreement with the predicted value for the thickness of the lipid bilayer and 10 Å larger than the thickness of the detergent belt (Figure 9B).[70,71,65] As mentioned above, the orientation of the 2-acetyl groups of P, which primarily influence the position of the P-band, can systematically be altered by the local electrostatics if hydrophobic residues near P are replaced with charged ones or the nature of the detergent is altered.[48,49] Besides the membrane lipids three integral lipid molecules were identified in one of the detergent-based structures in *Rba. sphaeroides* that most likely influence the rate of the electron transfer and contribute to the energetics of the unidirectional charge separation in the RC.[73] Of these three lipids cardiolipin was also resolved in the lipid-based structure.[72] Even though the polar headgroup of the cardiolipin is over 15 Å away from the closest cofactor, it is largely exposed and stabilized primarily by electrostatic interactions with Arg M267, His M145, and several water molecules. The cardiolipin was also proposed to be in contact with the membrane exposed surfaces of the H and M subunits.[74] Thus, the influence of cardiolipin would most likely be different in RCs isolated in detergents and in liposomes as it interacts with different hydrophobic chains. The observed differences in LDAO and in DLPC may also be addressed in terms of the stabilizing effect of the dipole potential of the lipid bilayer in DLPC. Studies are in progress to test the influence of the membrane dipole potential, for example by the addition of cholesterol, which increases the dipole potential in RCs from *Rba. sphaeroides*.[75]

These results revealed that the conformations of the dimer in the isolated RCs of *Rba. sphaeroides* and *Rba. capsulatus* in zwitterionic LDAO micelles are essentially the same in the dark-adapted samples as indicated by the identical wavelength of the dimer band at 865 nm. The same position is measured for RCs in their native membrane environments and in liposomes with long (C_{18}) hydrophobic chain lengths. The band is blue-shifted in *Rba. capsulatus*, but not in *Rba sphaeroides*, for RCs in zwitterionic detergent micelles and liposomes with short hydrophobic chains upon illumination. The P-band for RCs from *Rba. capsulatus* was observed at 850 nm and thought to be irreversible, but these results show that the two spectral forms of P can interconvert with the proper selection of detergent or lipid and also by using light as a switch. The two optical states also have different redox potentials and lifetimes of the charge-separated state in addition to the previously reported differences in the distribution of the unpaired electron of P^+.

The electronic state of P is very sensitive to the properties of the lipids and detergents that surround the protein and demonstrates the utility of the RC as a model system for membrane proteins. Alteration of the native lipid environment has a significant effect on P, including the energetics of the excited and oxidized states that are critical for the function. In addition to the previously identified influence of electrostatic interactions, hydrophobic interactions have a critical role in establishing the properties of P. In particular, the hydrophobic mismatch between the thickness of the detergent micelle and the length of the transmembrane helices is most likely responsible for the reported functional differences of the RC in detergent micelles, liposomes, and natural membranes.[13−16,19] These effects are expected to be general for all integral membrane proteins, in particular the properties of the primary electron donor of photosystem II.

AUTHOR INFORMATION

Corresponding Author

*Phone: 514-848-2424 x5051. Fax: 514-848-2828. E-mail: laszlo.kalman@concordia.ca.

Funding Sources

This work was supported by grants from Natural Sciences and Engineering Research Council of Canada (to L.K.) and from National Science Foundation (MCB 0640002 to J.P.A.).

ABBREVIATIONS

RC, reaction center; P, bacteriochlorophyll dimer; Q_A, primary quinone; Q_B, secondary quinone; *Rba*, *Rhodobacter*; DAD, 2,3,5,6-tetramethyl-*p*-phenylenediamine; LDAO, *N*-lauryl-*N*,*N*-dimethylamine-*N*-oxide; CTAB, cetyltrimethylammonium bromide; TX-100, Triton X-100; DOC, deoxycholate; DOPC, 1,2-dioleoyl-*sn*-glycero-3-phosphocholine; DOTAP, 1,2-dioleoyl-3-trimethylammonium−propane; DOPS, 1,2-dioleoyl-*sn*-glycero-3-phospho-L-serine; DLPC, 1,2-dilauroyl-*sn*-glycero-3-phosphocholine; C_{12} and C_{18}, fatty acid chains with 12 and 18 carbon atoms, respectively.

REFERENCES

(1) Hunter, C. N., Daldal, F., Thurnauer, M. C., and Beatty, J. T., Eds. (2008) *The Purple Phototropic Bacteria*, Springer-Verlag, Dordrecht, The Netherlands.

(2) Allen, J. P., Feher, G., Yeates, T. O., Komiya, H., and Rees, D. C. (1987) Structure of the reaction center from *Rhodobacter sphaeroides* R-26: The cofactors. *Proc. Natl. Acad. Sci. U.S.A. 84*, 5730–5734.

(3) Williams, J. C., Steiner, L. A., Ogden, R. C., Simon, M. I., and Feher, G. (1983) Primary structure of the M subunit of the reaction center from *Rhodopseudomonas sphaeroides*. *Proc. Natl. Acad. Sci. U.S.A. 80*, 6505–6509.

(4) Williams, J. C., Steiner, L. A., Feher, G., and Simon, M. I. (1984) Primary structure of the L subunit of the reaction center from *Rhodopseudomonas sphaeroides*. *Proc. Natl. Acad. Sci. U.S.A. 81*, 7303–7307.

(5) Youvan, D. C., Alberti, M., Begusch, H., Bylina, E. J., and Hearst, J. E. (1984) Reaction center and light-harvesting I genes from *Rhodopseudomonas capsulata*. *Proc. Natl. Acad. Sci. U.S.A. 81*, 189–192.

(6) Komiya, H., Yeates, T. O., Rees, D. C., Allen, J. P., and Feher, G. (1988) Structure of the reaction center from *Rhodobacter sphaeroides* R-26 and 2.4.1: Symmetry relations and sequence comparisons between different species. *Proc. Natl. Acad. Sci. U.S.A. 85*, 9012–9016.

(7) Kirmaier, C., and Holten, D. (1987) Primary photochemistry of reaction centers from the photosynthetic purple bacteria. *Photosynth. Res. 13*, 225–230.

(8) Marcus, R. A., and Sutin, N. (1985) Electron transfers in chemistry and biology. *Biochim. Biophys. Acta 811*, 265–322.

(9) Woodbury, N. W., and Allen, J. P. (1995) The pathway, kinetics and thermodynamics of electron transfer in wild type and mutant reaction centers of purple nonsulfur bacteria. *Anoxygenic Photosynthetic Bacteria* (Advances in Photosynthesis and Respiration) 2nd ed., pp 527−553, Kluwer Academic Publisher, Dordrecht, The Netherlands.

(10) Clayton, R. K. (1978) Effects of dehydration on reaction centers from *Rhodopseudomonas sphaeroides*. *Biochim. Biophys. Acta 504*, 255–264.

(11) Debus, R. J., Feher, G., and Okamura, M. Y. (1985) LM complex of reaction centers from *Rhodopseudomonas sphaeroides* R-26 characterization and reconstitution with the H-subunit. *Biochemistry 24*, 2488–2500.

(12) Eastman, J. E., Taguchi, A. K. W., Lin, S., Jackson, J. A., and Woodbury, N. W. (2000) Characterization of a *Rhodobacter capsulatus* reaction center mutant that enhances the distinction between spectral forms of the initial electron donor. *Biochemistry 39*, 14787–14798.

(13) Tiede, D. M., Vázquez, J., Córdova, J., and Marone, P. (1996) Time-resolved electrochromism associated with the formation of quinone anions in the *Rhodobacter sphaeroides* R26 reaction center. *Biochemistry 35*, 10763–10775.

(14) Lavergne, J., Matthews, C., and Ginet, N. (1999) Electron and proton transfer on the acceptor side of the reaction center in chromatophores of *Rhodobacter capsulatus*: Evidence for direct protonation of the semiquinone state of Q_B. *Biochemistry 38*, 4542–4552.

(15) Asztalos, E., and Maróti, P. (2009) Export or recombination of charges in reaction centers in intact cells of photosynthetic bacteria. *Biochim. Biophys. Acta 1787*, 1444–1450.

(16) Maróti, P. (1991) Electron transfer and proton uptake of photosynthetic reaction centers reconstituted in phospholipid vesicles. *J. Photochem. Photobiol. B 8*, 263–277.

(17) Maróti, P., and Wraight, C. A. (1988) Flash-induced H^+ binding by bacterial photosynthetic reaction centers: Influences of the redox states of the acceptor quinones and primary dimer. *Biochim. Biophys. Acta 934*, 329–347.

(18) McPherson, P. H., Okamura, M. Y., and Feher, G. (1988) Light-induced proton uptake by photosynthetic reaction centers from *Rhodobacter sphaeroides* R-26.1. Protonation of the one-electron states $D^+Q_A^-$, DQ_A^-, $D^+Q_AQ_B^-$, and $DQ_AQ_B^-$. *Biochim. Biophys. Acta 934*, 348–368.

(19) Tandori, J., Miksovska, J., Valerio-Lepiniec, M., Schiffer, M., Maróti, P., Hanson, D. K., and Sebban, P. (2002) Proton uptake of *Rhodobacter capsulatus* reaction center mutants modified in the primary quinone environment. *Photochem. Photobiol. 75*, 126–133.

(20) Goushcha, A. O., Kharkyanen, V. N., and Holzwarth, A. R. (1997) Nonlinear light-induced properties of photosynthetic reaction centers under low intensity irradiation. *J. Phys. Chem. B 101*, 259–265.

(21) Kálmán, L., and Maróti, P. (1997) Conformation-activated protonation in reaction center of the photosynthetic bacterium *Rhodobacter sphaeroides*. *Biochemistry 36*, 15269–15276.

(22) van Mourik, F., Reus, M., and Holzwarth, A. R. (2001) Long-lived charge separated states in bacterial reaction centers isolated from *Rhodobacter sphaeroides*. *Biochim. Biophys. Acta 1504*, 311–318.

(23) Xu, Q., and Gunner, M. R. (2001) Trapping conformational Intermediate States in the reaction center protein from photosynthetic bacteria. *Biochemistry 40*, 3232–3241.

(24) Andréasson, U., and Andréasson, L. E. (2003) Characterization of a semi-stable charge-separated state in reaction centers from *Rhodobacter sphaeroides*. *Photosynth. Res. 75*, 223–233.

(25) Olenchuk, M., and Berezetska, N. (2008) Study of the recombination process of light-induced charge separation in reaction centers of purple bacteria under long-term exposition. *Mol. Cryst. Liq. Cryst. 497*, 121–128.

(26) Stowell, M. H. B., McPhillips, T. M., Rees, D. C., Soltis, S. M., Abresch, E., and Feher, G. (1997) Light-induced structural changes in photosynthetic reaction center: Implications for mechanism of electron-proton transfer. *Science 276*, 812–816.

(27) Deshmukh, S. S., Williams, J. C., Allen, J. P., and Kálmán, L. (2011) Light-induced conformational changes in photosynthetic reaction centers: Dielectric relaxation in the vicinity of the dimer. *Biochemistry 50*, 340–348.

(28) Deshmukh, S. S., Williams, J. C., Allen, J. P., and Kálmán, L. (2011) Light-induced conformational changes in photosynthetic reaction centers: Redox-regulated proton pathway near the dimer. *Biochemistry 50*, 3321–3331.

(29) Wang, S., Lin, S., Lin, X., Woodbury, N. W., and Allen, J. P. (1994) Comparative study of reaction centers from purple photosynthetic bacteria: Isolation and optical spectroscopy. *Photosynth. Res. 42*, 203–215.

(30) Müh, F., Rautter, J., and Lubitz, W. (1997) Two distinct conformations of the primary electron donor in reaction centers from *Rhodobacter sphaeroides* revealed by ENDOR/TRIPLE-spectroscopy. *Biochemistry 36*, 4155–4162.

(31) Youvan, D. C., Ismail, S., and Bylina, E. J. (1985) Chromosomal deletion and plasmid complementation of the photosynthetic reaction center and light-harvesting genes from *Rhodopseudomonas capsulatus*. *Gene 38*, 19–30.

(32) Bylina, E. J., Ismail, S., and Youvan, D. C. (1986) Plasmid pU29, a vehicle for mutagenesis of the photosynthetic *puf* operon in *Rhodopseudomonas capsulata*. *Plasmid 16*, 175–181.

(33) Bylina, E. J., and Youvan, D. C. (1988) Directed mutations affecting spectroscopic and electron transfer properties of the primary donor in the photosynthetic reaction center. *Proc. Natl. Acad. Sci. U.S.A. 85*, 7226–7230.

(34) Weaver, P. F., Wall, J. D., and Gest, H. (1975) Characterization of *Rhodopseudomonas capsulate*. *Arch. Microbiol. 105*, 207–216.

(35) Williams, J. C., Alden, R. G., Murchison, H. A., Peloquin, J. M., Woodbury, N. W., and Allen, J. P. (1992) Effects of mutations near the bacteriochlorophylls in reaction center from *Rhodobacter sphaeroides*. *Biochemistry 31*, 11029–11037.

(36) Olivon, M., Lesiur, S., Gabrielle-Madelmount, C., and Paternostre, M. (2000) Vesicle reconstitution from lipid-detergent mixed micelles. *Biochim. Biophys. Acta 1508*, 34–50.

(37) Moss, D. A., Leonhard, M., Bauscher, M., and Mäntele, W. (1991) Electrochemical redox titration of cofactors in the reaction center from *Rhodobacter sphaeroides*. *FEBS Lett. 283*, 33–36.

(38) O'Reilly, J. E. (1973) Oxidation-reduction potential of the ferro-ferricyanide system in buffer solutions. *Biochim. Biophys. Acta 292*, 509–515.

(39) Lin, X., Murchison, H. A., Nagarajan, V., Parson, W. W., Allen, J. P., and Williams, J. C. (1994) Specific alteration of the oxidation potential of the electron donor in reaction centers from *Rhodobacter sphaeroides*. *Proc. Natl. Acad. Sci. U.S.A. 91*, 10265–10269.

(40) Parson, W. W. (2007) Electronic absorption in *Modern Optical Spectroscopy*, pp 182−188, Springer-Verlag, Berlin, Germany.

(41) Clayton, R. K. (1980) *Photosynthesis: Physical Mechanisms and Chemical Patterns*, Cambridge University Press, New York.

(42) Dutton, P. L., and Jackson, J. B. (1972) Thermodynamic and kinetic characterization of electron transfer components *in situ* in *Rhodopseudomonas sphaeroides* and *Rhodospirillum rubrum*. *Eur. J. Biochem. 30*, 495–510.

(43) Osváth, S., and Maróti, P. (1997) Coupling of cytochrome and quinone turnovers in the photocycle of reaction centers from the photosynthetic bacterium *Rhodobacter sphaeroides*. *Biophys. J. 73*, 972–982.

(44) Kálmán, L., Haffa, A. L. M., Williams, J. C., Woodbury, N. W., and Allen, J. P. (2007) Reduction of the oxidized bacteriochlorophyll dimer in reaction centers by ferrocene is dependent upon the driving force. *J. Porphyrins Phthalocyanines 11*, 205–211.

(45) Kleinfeld, D., Abresch, E. C., Okamura, M. Y., and Feher, G. (1984) Damping of oscillations in the semiquinone absorption in reaction centers after successive flashes. Determination of the equilibrium between $Q_A^-Q_B$ and $Q_AQ_B^-$. *Biochim. Biophys. Acta 765*, 406–409.

(46) Rautter, J., Lendzian, F., and Lubitz, W. (1994) Comparative study of reaction centers from photosynthetic purple bacteria: Electron Paramagnetic Resonance and Electron Nuclear Double Resonance Spectroscopy. *Biochemistry 33*, 12077–12084.

(47) Plato, M., Lendzian, F., Lubitz, W., and Mobius, K. (1992) Molecular orbital study of electronic asymmetry in primary donors of bacterial reaction centers. *Photosynth. Bact. React. Cent. II 237*, 109–118.

(48) Rautter, J., Lendzian, F., Shulz, C., Fetsch, A., Kuhn, M., Lin, X., Williams, J. C., Allen, J. P., and Lubitz, W. (1995) ENDOR studies of the primary donor cation radical in mutant reaction centers of *Rhodobacter sphaeroides* with altered hydrogen-bond interactions. *Biochemistry 34*, 8130–8143.

(49) Müh, F., Schulz, C., Schlodder, E., Jones, M. R., Rautter, J., Kuhn, M., and Lubitz, W. (1998) Effects of zwitterionic detergents on the electronic structure of the primary donor and the charge recombination kinetics of $P^+Q_A^-$ in native and mutant reaction centers from *Rhodobacter sphaeroides*. *Photosynth. Res. 55*, 199–205.

(50) Kuglstatter, A., Hellwig, P., Fritzsch, G., Wachtveitl, J., Oesterhelt, D., Mäntele, W., and Michel, H. (1999) Identification of a hydrogen bond in the Phe M197→ Tyr mutant reaction center of the photosynthetic purple bacterium *Rhodobacter sphaeroides* by X-ray crystallography and FTIR spectroscopy. *FEBS Lett. 463*, 169–174.

(51) Wachtveitl, J., Farchaus, J. W., Das, R., Lutz, M., Robert, B., and Mattioli, T. A. (1993) Structure, spectroscopic, and redox properties of *Rhodobacter sphaeroides* reaction centers bearing point mutations near the primary electron donor. *Biochemistry 32*, 12875–12886.

(52) Mattioli, T. A., Sockalingum, D., Lutz, M., and Robert, B. (1992) Low temperature Fourier transform resonance Raman spectroscopy of the primary donor in *Rhodobacter sphaeroides*. *Res. Photosynth., Proc. Int. Congr. Photosynth., 9th 1*, 405–408.

(53) Mattioli, T. A., Lin, X., Allen, J. P., and Williams, J. C. (1995) Correlation between multiple hydrogen bonding and alteration of the oxidation potential of the bacteriochlorophyll dimer of *Rhodobacter sphaeroides*. *Biochemistry 34*, 6142–6152.

(54) Nagarajan, V., Parson, W. W., Davis, D., and Schenck, C. C. (1993) Kinetics and free-energy gaps of electron-transfer reactions in *Rhodobacter sphaeroides* reaction centers. *Biochemistry 32*, 12324–12336.

(55) Ermler, U., Fritzsch, G., Buchanan, S. K., and Michel, H. (1994) Structure of the photosynthetic reaction center from *Rhodobacter sphaeroides* at 2.65 Å resolution. Cofactors and protein-cofactor interactions. *Structure 2*, 925–936.

(56) Ginet, N., and Lavergne, J. (2000) Interactions between the donor and acceptor sides in bacterial reaction centers. *Biochemistry 39*, 16252–16262.

(57) Lancaster, C. R. D. (1998) Ubiquinone reduction and protonation in photosynthetic reaction centres from *Rhodopseudomonas viridis*: X-ray structures and their functional implications. *Biochim. Biophys. Acta 1365*, 143–150.

(58) Lancaster, C. R. D., and Michel, H. (1999) Refined crystal structures of reaction centres from *Rhodopseudomonas viridis* in complexes with the herbicide atrazine and two chiral atrazine derivatives also lead to a new model of the bound carotenoid. *J. Mol. Biol. 286*, 883–898.

(59) Allen, J. P., Lous, E. J., Feher, G., Chirino, A., Komiya, H., and Rees, D. C. (1990) Structure of the reaction center from *Rhodobacter sphaeroides*: Further refinement of R-26 and 2.4.1 structures and interactions between the reaction center and herbicides. *Curr. Res. Photosynth., Proc. Int. Conf. Photosynth., 8th*.

(60) Brzezinski, P., Okamura, M. Y., and Feher, G. (1992) Structural change following the formation of $D^+Q_A^-$ in bacterial reaction centers: Measurement of light-induced electrogenic events in reaction centers incorporated in a phospholipid monolayer. *Photosynth. Bact. React. Cent. II 237*, 321–330.

(61) Kálmán, L., Turzó, K., and Maróti, P. (1993) Probing reaction center protonation by electrochromic absorption changes of cofactors in *Rhodobacter sphaeroides*. *Photosynthetica 28*, 185–194.

(62) Tiede, D. M., and Hanson, D. K. (1992) Protein relaxation following quinone reduction in *Rhodobacter capsulatus*: Detection of likely protonation linked optical absorbance changes of the chromophores. *Photosynth. Bact. React. Cent. II* 341–350.

(63) Williams, J. C., Haffa, A. L. M., McCulley, J. L., Woodbury, N. W., and Allen, J. P. (2001) Electrostatic interactions between charged amino acid residues and the bacteriochlorophyll dimer in reaction centers from *Rhodobacter sphaeroides*. *Biochemistry 40*, 15403–15407.

(64) Agostiano, A., Milano, F., and Trotta, M. (2005) Trapping of a long-living charge separated state of photosynthetic reaction centers in proteoliposomes of negatively charged phospholipids. *Photosynth. Res. 83*, 53–61.

(65) Roth, M., Arnoux, B., Ducruix, A., and Reiss-Husson, F. (1991) Structure of the detergent phase and protein-detergent interactions in crystals of the wild-type (strain Y) *Rhodobacter sphaeroides* photochemical reaction center. *Biochemistry 30*, 9403–9413.

(66) Arnoux, B., Gaucher, J. F., Ducruix, A., and Reiss-Husson, F. (1995) Structure of the photochemical reaction center of a spheroidine containing purple bacterium *Rhodobacter sphaeroides* Y at 3 Angstroms resolution. *Acta Crystallogr., Sect. D: Biol. Crystallogr. 51*, 368–379.

(67) Bowie, J. U. (2005) Solving the membrane protein folding problem. *Nature 438*, 581–589.

(68) Killian, J. A. (1998) Hydrophobic mismatch between proteins and lipids in membranes. *Biochim. Biophys. Acta 1376*, 401–416.

(69) Wood, B. J. B., Nichols, B. W., and James, A. T. (1965) The lipids and fatty acid metabolism of photosynthetic bacteria. *Biochim. Biophys. Acta 106*, 261–273.

(70) Donohue, T. J., Chain, B. D., and Kaplan, S. (1982) Alteration of the phospholipid composition of *Rhodopseudomonas sphaeroides* and other bacteria by Tris. *J. Bacteriol. 152*, 595–606.

(71) Dumas, F., Lebrun, M. C., and Tocanne, J. F. (1999) Is the protein/lipid hydrophobic matching principle relevant to membrane organization and functions? *FEBS Lett. 458*, 271–277.

(72) Katona, G., Andréasson, U., Landau, E. M., Andréasson, L. E., and Neutze, R. (2003) Lipidic cubic phase crystal structure of the photosynthetic reaction center from *Rhodobacter sphaeroides* at 2.35 Å resolution. *J. Mol. Biol. 331*, 681–692.

(73) Camara-Artigas, A., Brune, D., and Allen, J. P. (2002) Interactions between lipids and bacterial reaction centers determined by protein crystallography. *Proc. Natl. Acad. Sci. U.S.A. 99*, 11055–11060.

(74) McAuley, K. E., Feyfe, P. K., Ridge, J. P., Isaacs, N. W., Cogdell, R. J., and Jones, M. R. (1999) Structural details of interaction between cardiolipin and an integral membrane protein. *Proc. Natl. Acad. Sci. U.S.A. 96*, 14706–14711.

(75) Pilotelle-Bunner, A., Beaunier, P., Tandori, J., Maróti, P., Clarke, R. J., and Sebban, P. (2009) The local electric field within phospholipid membranes modulates the charge transfer reactions in reaction centres. *Biochim. Biophys. Acta 1787*, 1039–1049.